$p93^{dis1}$, which is required for sister chromatid separation, is a novel microtubule and spindle pole body-associating protein phosphorylated at the Cdc2 target sites

Kentaro Nabeshima, Hisanori Kurooka,[1] Masahiro Takeuchi,[2] Kazuhisa Kinoshita, Yukinobu Nakaseko, and Mitsuhiro Yanagida[3]

Department of Biophysics, Faculty of Science, Kyoto University,

Kitashirakawa-Oiwakecho, Sakyo-ku, Kyoto 606, Japan

Fission yeast cold-sensitive (cs) *dis1* mutants are defective in sister chromatid separation. The *dis1*$^+$ gene was isolated by chromosome walking. The null mutant showed the same phenotype as that of cs mutants. The *dis1*$^+$ gene product was identified as a novel 93-kD protein, and its localization was determined by use of anti-dis1 antibodies and green fluorescent protein (GFP) tagged to the carboxyl end of $p93^{dis1}$. The tagged $p93^{dis1}$ in living cells localizes along cytoplasmic microtubule arrays in interphase and the elongating anaphase spindle in mitosis, but association with the short metaphase spindle microtubules is strikingly reduced. In the spindle, the tagged $p93^{dis1}$ is enriched at the spindle pole bodies (SPBs). Time-lapse video images of single cells support the localization shift of $p93^{dis1}$ to the SPBs in metaphase and spindle microtubules in anaphase. The carboxy-terminal fragment, which is essential for Dis1 function, accumulates around the mitotic SPB. We propose that these localization shifts of $p93^{dis1}$ in mitosis facilitates sister chromatid separation by affecting SPB and anaphase spindle function.

[*Key Words*: Cell cycle; microtubule; spindle pole body; Cdc2 kinase; fission yeast; chromosome segregation]

Received February 6, 1995; revised version accepted May 31, 1995.

Microtubules and chromosomes undergo dramatic structural changes during the cell division cycle. Microtubules that have intrinsic dynamic instability (Mitchison and Kirschner 1984; Walker et al. 1988) transform between the cytoplasmic network in interphase and the spindle apparatus in mitosis (e.g., Hagan and Hyams 1988). The interphase network is rapidly disassembled, followed by reassembly into the mitotic spindle. At the end of mitosis, the spindle is disassembled, and the cytoplasmic microtubule network reorganizes.

Kinases and phosphatases regulate the dynamics and steady-state length of microtubules (Belmont et al. 1990; Verde et al. 1992; Vandre and Willis 1992; Gliksman et al. 1992). The severing of microtubules is another mechanism for destabilizing and disassembling the microtubule network (Vale 1991; Verde et al. 1992; McNally and Vale 1993; Shiina et al. 1994). The severing activity found in *Xenopus* egg extracts can be activated by addition of either cyclin B or A or Cdc2 kinase, which plays a crucial role in the transition from interphase to mitosis (Nurse 1990).

Microtubule-organizing centers (MTOCs) play an essential role in nucleating microtubule assembly and forming the microtubule array. In interphase cells, microtubules are nucleated and polarized in the cytoplasm by centrosome (Bergen et al. 1980; Heidemann and McIntosh 1980). Centrosomes duplicate upon entry into mitosis and become the spindle poles, which radiate polar microtubules. In yeast, the centrosome equivalent spindle pole body (SPB) plays a role similar to that of the centrosome. A large number of yeast genes and their products have been shown to be involved in SPB function (Snyder 1994). They may be classified into two groups, SPB components and components associated with the SPB.

The fission yeast *Schizosaccharomyces pombe* is an excellent model organism for studying microtubule dy-

Present addresses: [1]Department of Medical Chemistry, Faculty of Medicine, Kyoto University, Sakyo-ku, Kyoto 606, Japan; [2]Tularik, Inc., South San Francisco, California 94080 USA.
[3]Corresponding author.

namics in the cell cycle. The microtubule structural change in *S. pombe* from interphase to mitosis and from mitosis to interphase is rapid and highly similar to that of higher eukaryotes (McCully and Robinow 1971; Tanaka and Kanbe 1986; Hagan and Hyams 1988; Masuda et al. 1992; Funabiki et al. 1993). During interphase, microtubule arrays run from one end of a cell to the other. Upon entry into mitosis, these cytoplasmic microtubules are rapidly disassembled and the SPBs are duplicated. The spindle, which runs between the duplicated SPBs, forms within the nucleus (e.g., Hagan and Yanagida 1992). At the time of metaphase/anaphase transition, condensed chromosomes are arranged at the middle of the short spindle (Funabiki et al. 1993). Anaphase A (sister chromatid separation) occurs without an accompanying increase in the pole-to-pole distance, while spindle elongation during anaphase B leads to a severalfold increase in the pole-to-pole distance. The metaphase spindle consists of polar microtubules, the number of which is severalfold more than that in the elongating anaphase spindle (Ding et al. 1993). Astral microtubules emanating from both SPBs are found only in the elongating anaphase spindle (Hagan and Hyams 1988). After the completion of anaphase, the fully extended spindle microtubules become disassembled and the cytoplasmic microtubule arrays rapidly reform from the MTOCs, which appear at the equator of the dividing cell (Hagan and Hyams 1988; Horio et al. 1991). This stage, after nuclear division and before cytokinesis, is called postanaphase.

In G_2-arrested mutants such as *cdc2* or *cdc25*, in which Cdc2 kinase is not activated, the cytoplasmic microtubule network remains in elongated cells. In metaphase-arrested mutants containing activated Cdc2 kinase, this network disappears and the short metaphase spindle forms (Stone et al. 1993). Neither spindle elongation nor sister chromatid separation occurs in these metaphase-arrested mutants.

Cold-sensitive (cs) *dis1* mutants are defective in sister chromatid separation at the restrictive temperature (Ohkura et al. 1988). Mutant cells enter mitosis with seemingly normal spindle formation and chromosome condensation. This is followed by spindle elongation accompanied by poleward chromosome movement, but chromosomes never become separated, leading to an unequal distribution of condensed chromosomes at both cell ends. These cells contain high H1 kinase activity (Kinoshita et al. 1991a; Stone et al. 1993). Thus, *dis1* mutants remain in a mid-mitotic stage in regard to high H1 kinase activity and the lack of sister chromatid separation, but the spindle untimely elongates. High frequency losses of a minichromosome occur in *dis1* mutant cells at the permissive temperature (Ohkura et al. 1988).

Two other *dis* mutants, *dis2* and *dis3*, have similar phenotypes (Ohkura et al. 1988). Pairwise crosses indicated that all the double mutants among *dis1*, *dis2*, and *dis3* were lethal. The phenotypes of *dis2* and *dis3* were later found to be allele-specific (Ohkura et al. 1989; Kinoshita et al. 1991b). The *dis2*$^+$ gene encodes the catalytic subunit of a type 1 (PP1) protein serine/threonine phosphatase (Ohkura et al. 1989). PP1 activity in extracts of *dis2-11* mutant cells was greatly reduced (Kinoshita et al. 1990). The *dis3*$^+$ gene is essential for viability and encodes a 110-kD protein (Kinoshita et al. 1991b) that has a suppressor function for the loss of phosphatase Ppe1 (Shimanuki et al. 1993). Some phosphatase mutations in other organisms such as *Aspergillus nidulans* and *Drosophila* (Doonan and Morris 1989; Axton et al. 1990; Mayer-Jaekel et al. 1993) also undergo aberrant mitosis.

We addressed the question, What is the role of Dis1 protein in mitosis and, concomitantly, What is the primary defect in the *dis1* mutant. To approach the problem we attempted to isolate the *dis1*$^+$ gene and characterize the gene product.

Results

Isolation of the dis1$^+$ *gene*

To isolate the *dis1*$^+$ gene, plasmids containing *S. pombe* genomic DNAs that suppressed the *dis1* phenotype were isolated, but they contained only extragenic suppressor genes (Kinoshita et al. 1991a; Takeuchi and Yanagida 1993). Genetic analysis indicated that the *dis1* locus was linked to *ura4* on the left arm of chromosome III (40 cM to *ura4*). No known marker existed between *ura4* and *dis1*. Chromosome walking was applied to isolate the *dis1*$^+$ gene with the *ura4*$^+$ gene used as the initial probe. A cosmid clone that is 220 kb distant from the *ura4*$^+$ gene complemented the cs phenotype of *dis1* mutations (Materials and methods). An ~4-kb-long fragment subcloned from the cosmid rescued the cs phenotype of all the *dis1* mutants examined. The cloned gene was integrated onto the chromosome with the marker gene by homologous recombination. Genetic analysis of the integrants confirmed that the cloned DNA was tightly linked to the *dis1* locus.

The dis1$^+$ *gene encodes an 882-amino-acid protein*

Nucleotide sequencing indicated that the cloned *dis1*$^+$ gene encodes an 882-amino-acid protein (Fig. 1a). The coding region is interrupted by a putative 267-bp intron. No other open reading frame was found. cDNA clones were isolated from the *S. pombe* library (a gift of Dr. M. Wigler, Cold Spring Harbor Laboratory) by hybridization, and nucleotide sequencing of the cDNAs confirmed the presence of the intron (data not shown). An unusual property of the cDNA was its >1-kb-long 5′-noncoding sequence, which was shown, by genomic sequencing, not to be an artifactual ligation product.

The predicted amino acid sequence has no strong overall homology to known proteins in the data bases but displays several notable features. The amino-terminal half domain is significantly similar to the protein sequence predicted by a human cDNA (GenBank data base accession no. D43948) from immature myeloid cell line.

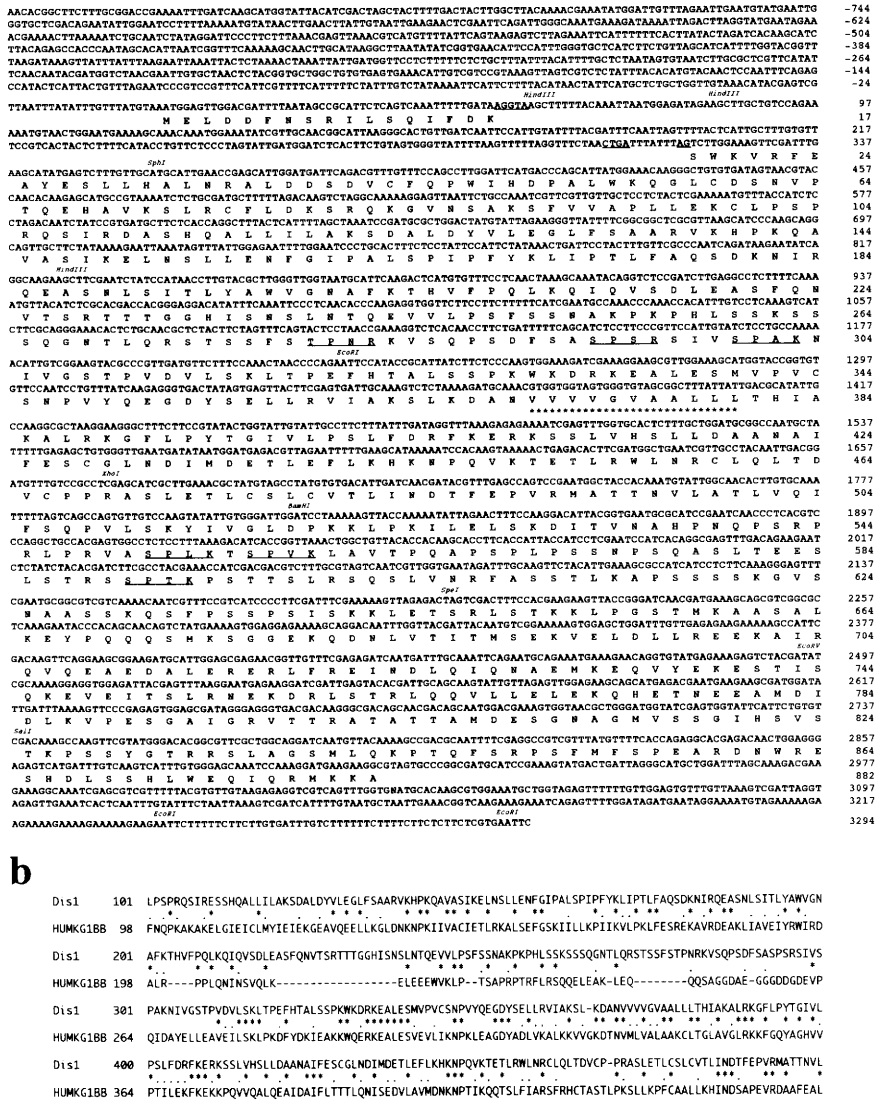

Figure 1. Nucleotide and predicted amino acid sequences of *dis1*$^+$. (*a*) Nucleotide sequence of the fission yeast *dis1*$^+$ gene, containing an intron (the consensus indicated by the underline) and encoding 882 amino acids. The Cdc2 kinase consensus (S/TPXK/R) is underlined. A hydrophobic sequence present in the amino-terminal domain is indicated by asterisks. The GenBank accession no. is D55635. (*b*) Identical amino acids between Dis1 and the predicted sequence of a human cDNA (HUMKG1BB; accession no. D43948) are shown by asterisks (similar amino acids are in dots).

Identical residues (29.2% over 290 amino acids) are indicated in Figure 1. An ~120 amino-acid-long region (amino acids 541–657) rich in proline, serine, threonine, and basic amino acids (totaling 66%) is present in the central domain. Six phosphorylation targets T/SPXK/R for Cdc2 kinase are clustered in the amino-terminal half (amino acids 278–303) and the central region (amino acids 550–593). The carboxy-terminal region is strongly hydrophilic.

Similarity of gene disruption phenotype to that of cs dis *mutants*

The chromosomal *dis1*$^+$ gene was disrupted by integration of linearized plasmids with the marker gene *S. pombe ura4*$^+$ (Materials and methods); a plasmid construct lacking most of the *dis1*$^+$ gene was made and used for gene disruption. Southern hybridization verified that the *dis1*$^+$ gene was disrupted in the heterozygous diploids (data not shown). For all integrants of plasmid constructs, only two viable spores, which were Ura$^-$, were obtained at 22°C; Ura$^+$ spores did not form colonies. However, all four spores were viable at 33°C, demonstrating that the gene disruptions were cs like the originally isolated *dis1* mutants. Thus, the *dis1*$^+$ gene is not absolutely required for viability.

Micrographs of *dis1* deletion mutant cells germinated at 33°C or 20°C and stained by DAPI and anti-tubulin antibody are shown in Figure 2a. The phenotype was indistinguishable from that of cs *dis1* mutants at 20°C. The mitotic spindle was elongated; and along it, the condensed chromosomes migrated to the poles in the absence of sister chromatid separation, resulting in the unequal distribution at the two cell ends. In the terminally arrested cells, the microtubules formed a V-like wedge-shaped structure in association with the condensed chromosomes. This V-shaped structure was also seen in cs *dis1*-mutant cells (Ohkura et al. 1988).

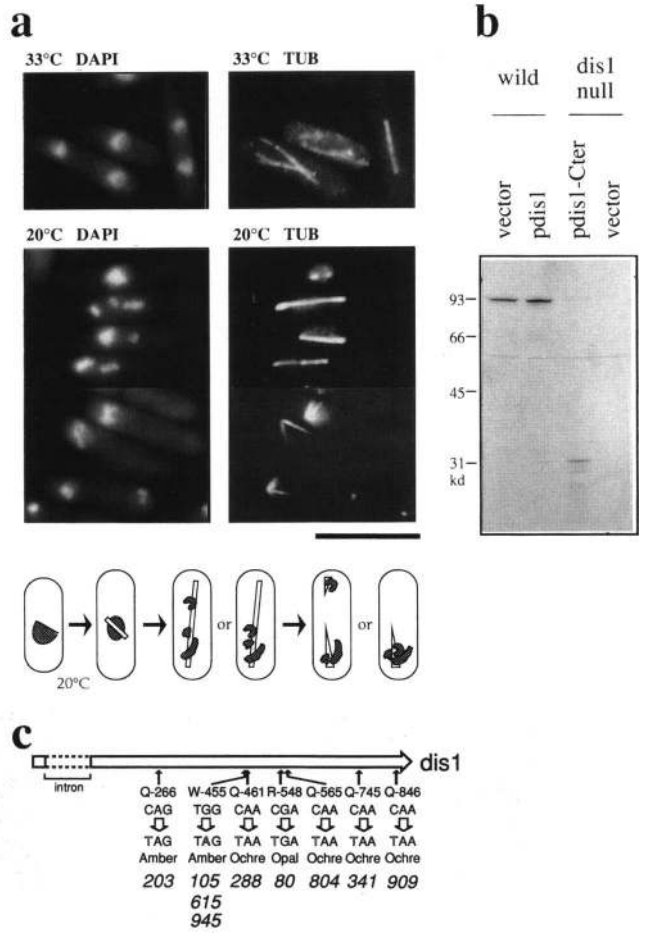

Figure 2. Gene disruption phenotype and protein identification. (*a*) Cells of the *dis1* gene disruptant were cultured at 20°C and 33°C, and stained by DAPI and monoclonal anti-tubulin antibodies (TAT1; Woods et al. 1989). At 33°C, normal cells were observed, whereas at 20°C aberrant mitotic cells were seen. The short, often V-shaped spindle ends were associated with the chromosomes. The phenotype of *dis1* gene disruption cells at 20°C is depicted schematically. Bar, 10 μm. (*b*) Identification of Dis1 protein in *S. pombe* extracts by immunoblot with anti-dis1 antibodies. (Lane *1*) Wild-type cells carrying vector plasmid; (lane *2*) wild-type cells carrying pdis1 with the *dis1*$^+$ gene; (lane *3*) *dis1* gene disruptant cells carrying pdis1–Cter; (lane *4*) *dis1* null mutant cells carrying vector plasmid. The 93-kD polypeptide was detected in lanes *1* and *2* . The 31-kD carboxy-terminal polypeptide was produced in lane *3*. The ~60-kD band present in all of the lanes was a contaminating antigen. (*c*) Mutation sites of nine cs *dis1* strains were determined by the integration rescue followed by PCR cloning and sequencing. They were all nonsense mutations. *dis1-203*, e.g., contained the mutation at codon 266, from CAG to TAG, causing the amber codon from the codon for Q (Gln).

Identification of p93 as the product of dis1$^+$ *gene*

To identify the Dis1 protein in *S. pombe* extracts, rabbit antiserum was raised against the carboxy-terminal fusion protein and used for immunoblot (Fig. 2b). The 93-kD polypeptide was detected in wild-type extracts carrying the vector plasmid (lane 1) and the multicopy plasmid pdis1 with the full-length *dis1*$^+$ gene (lane 2). The band intensity of p93 was increased two- to three-fold by pdis1. The calculated molcular mass of Dis1 protein was 97.6 kD. The 93-kD band was not observed in *dis1* null mutant (lane 4). From these results we concluded that p93 is the product of *dis1*$^+$ gene.

Location and nature of mutation sites

In our previous screening, a number of *dis1* alleles were obtained (9 of 982 cs strains examined; Ohkura et al. 1988). They showed basically the same phenotype. To understand the nature of cs *dis1* mutations, the approximate mutation sites were mapped by random spore analysis and integration rescue of the cs phenotype by truncated genes, followed by PCR amplification and sequencing of DNA clones that contained these sites. Surprisingly, all of the sites examined were nonsense mutations, distributed between codon 266 and 846 (Fig. 2c). Immunoblotting with antibodies against the amino-terminal domain showed fragments with a molecular mass consistent with the nonsense mutation sites in mutant cells (data not shown). These results strongly suggested that the carboxy-terminal domain was important for complementation of *dis1* mutants. A multicopy plasmid, pdis1–Cter, carrying the truncated gene coding for the carboxy-terminal 31-kD region (amino acids 658–882) was able to complement both cs and null mutants. By immunoblotting, a 31-kD polypeptide was detected in cells carrying pdis1–Cter (Fig. 2b, lane 3).

Immunolocalization of p93^{dis1} protein

Immunolocalization of p93^{dis1} was examined by use of affinity-purified anti-dis1 antibodies (dis1, Fig. 3). Exponentially growing wild-type (designated WT cells), wild-type cells carrying multicopy plasmid pDIS1 (designated OP), and *dis1* gene-disrupted cells (null) grown at the permissive temperature (33°C) were stained with anti-dis1 antibodies (against the 31-kD carboxy-terminal fragment; see Materials and methods), with TAT1 for microtubules, and with DAPI for nuclei.

Colocalization of anti-dis1 antibodies and microtubules was observed in wild-type cells. Staining was enhanced in plasmid-borne cells (OP) but was completely absent in gene-disrupted cells (null). Thus, microtubule staining must be attributable to the presence of the p93^{dis1} protein. In interphase and postanaphase cells, immunofluorescence was intense along the cytoplasmic microtubule arrays, which run between the two cell ends. In postanaphase cells containing two nuclei, X-shaped microtubules were clearly stained.

In mitotic cells containing the spindle, however, anti-dis1 staining was weak and variable from cell to cell. Two examples of mitotic cells are shown in Figure 3b. Aster microtubule, polar spindle microtubule, and possibly the SPB are seen. This weak staining is possibly a result of poor preservation of Dis1 protein in the spindle during specimen preparation, inaccessibility of the anti-

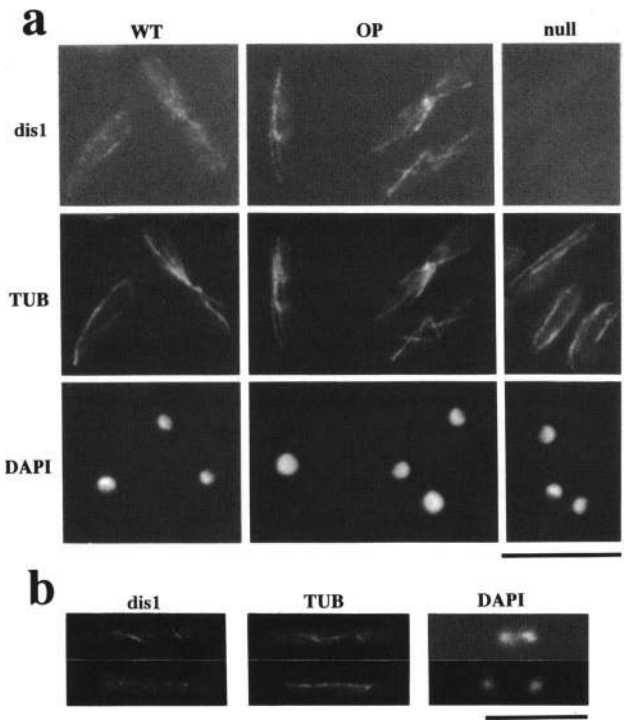

Figure 3. Colocalization of Dis1 protein with microtubules. (*a*) Micrographs of *S. pombe* stained by affinity-purified anti-dis1 (dis1; against the carboxy-terminal fragment) and anti-tubulin (TUB) antibodies. The same cells were also stained by DAPI. (WT) Wild-type cells: (OP) wild-type cells carrying multicopy plasmid with the *dis1*$^+$ gene: (null) *dis1* gene disrupted cells. Bar, 10 μm. (*b*) Wild-type mitotic cells stained by anti-dis1, and anti-tubulin antibodies and DAPI. Bar, 10 μm.

bodies to Dis1 in the spindle, or the lack of p93^{dis1} association with spindle microtubule.

Visualization of Dis1 protein tagged with green fluorescent protein

To further examine microtubule association of p93^{dis1}, we applied the tag of jellyfish green fluorescent protein (GFP) recently developed for visualizing proteins expressed with GFP (Chalfie et al. 1994); GFP has no bound ligand but can emit strong green fluorescence by absorbing blue or blue–violet excitation light. The GFP can be tagged to the carboxyl terminus of protein to visualize its localization in living cells. Plasmid carrying the coding region of GFP (a kind gift of Dr. M. Chalfie, U.S. Department of Agriculture, MA) was used to construct the plasmid pdis1–GFP, which carries the *dis1*$^+$ gene, the carboxyl terminus of which was ligated with the GFP sequence. Immunoblot of cells carrying the plasmid pdis1–GFP showed the band with the expected molecular mass (data not shown). GFP introduced into and expressed in *S. pombe* cells showed no toxic effect on the growth rate, and green fluorescence was seen to be homogeneously distributed in whole cells (Fig. 4d). The *dis1* deletion mutant cells grew completely normally at the restrictive temperature when the plasmid pdis1–GFP was introduced, indicating that GFP-bound Dis1 was functional. The *dis1* deletion mutant cells carrying pdis1–GFP were used for visualization of the GFP-tagged Dis1 protein.

In nonfixed living cells, green fluorescence is observed along microtubule structures (Fig. 4a): Cytoplasmic microtubule arrays characteristic of G_2 cells (indicated by I) and post-anaphase (PA) cells are clearly seen. These interphase cell types were abundant in exponentially growing cultures. Fluorescence is also visualized along the mitotic spindle-like structure (labeled A). As determined from its length (3–15 μm), it is likely to be the anaphase spindle (the metaphase spindles are short, ranging from 2.0 to 2.5 μm in length). Examples of several cells displaying green extended spindle structures are shown in Figure 4b. Green fluorescence is uniformly distributed along the elongating spindle except for the fully elongated ones, the central region of which is often dim.

Both spindle ends are intensely fluorescent, suggesting that p93^{dis1} is associated with the mitotic SPB as well as spindle microtubule. The aster microtubules (indicated by the small arrows in Fig. 4b), which appear in anaphase, also show green fluorescence.

In early mitotic (EM) or metaphase cells containing the short spindle structure, green fluorescence along microtubules between the poles was rather dim (Fig. 4a,c) in comparison with that in the elongating anaphase spindle. Instead, fluorescence was strong at the SPBs. On the basis of the consideration that the metaphase spindle consists of many more microtubules than that of anaphase (Ding et al. 1993), relative green fluorescence per microtubule would be significantly lower than that in the anaphase spindle. This suggests that association of p93^{dis1} may shift from the microtubules to the SPBs in metaphase.

Green fluorescence was consistently intense at the SPBs in metaphase-arrested *nuc2* mutant cells that carried the plasmid pdis1–GFP and were cultured at the restrictive temperature for 5 hr [Fig. 5a; anti-tubulin or anti-SPB antibody (Hagan and Yanagida 1995) stainings shown at right are controls]. The *nuc2* mutant cells were arrested at metaphase, displaying the short spindle (Hirano et al. 1988). Polar microtubules were also seen, but the relative intensity of green fluorescence was much less than that at the SPBs. As a control experiment plasmid carrying only GFP was expressed in *nuc2* mutant, and green fluorescence was found to be diffused in whole cells (see Fig. 7b, below).

A highly sensitive video camera (see Materials and methods) was employed to monitor the changes of green fluorescence in single mitotic cells. Continuous illumination of cells by blue light caused lethal damage to them. However, if cells were exposed to light very briefly at proper time intervals, green fluorescence displaying dynamic spindle behavior was visible for individual cells. An example of such monitored cells is shown in Figure 5b. Green fluorescence along the polar microtubule was minimal for the short spindle but then restored in the elongating spindle. The rate of spindle elongation was ~0.5 μm/min at room temperature (20°C) in a syn-

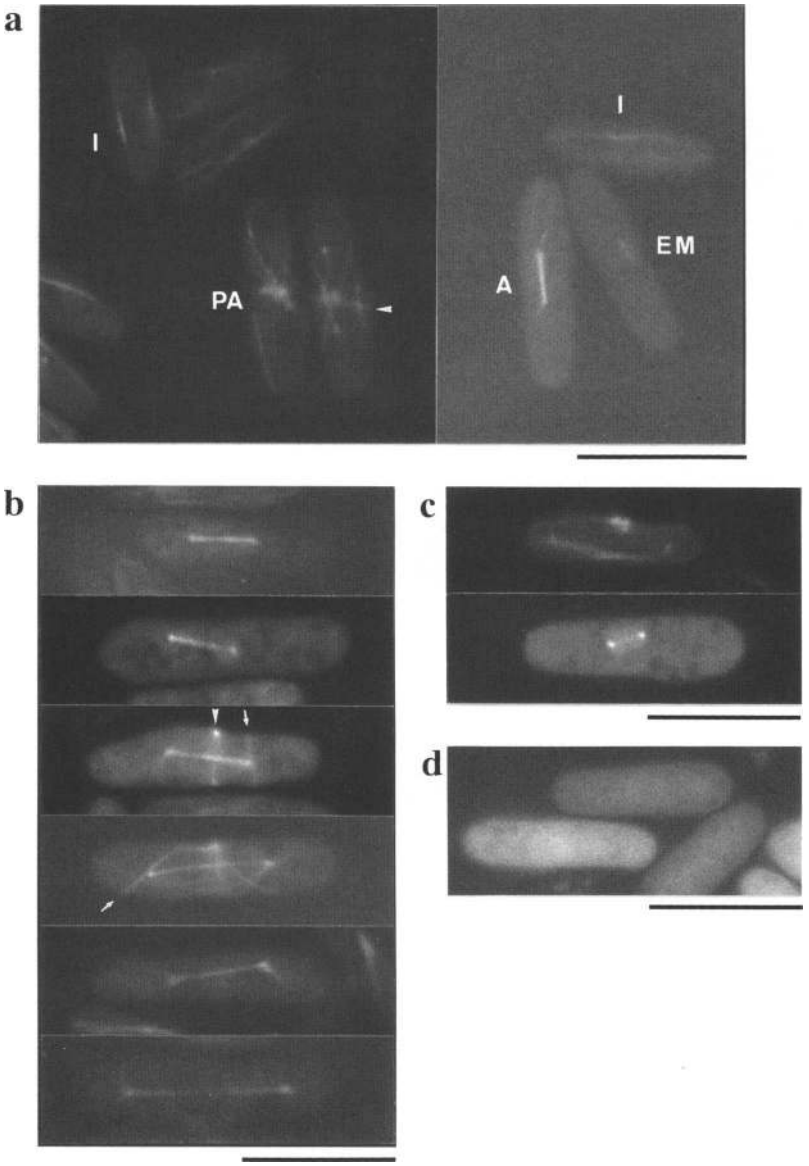

Figure 4. Localization of green fluorescent GFP-tagged Dis1 protein. (*a*) Green fluorescence in *S. pombe dis1*-deletion cells carrying the plasmid pdis1–GFP. Cells living in the culture medium were observed without fixation. Green fluorescence is observed along microtubule structures. Cytoplasmic arrays characteristic of G_2 cells (indicated by I) and postanaphase (PA), as well as the anaphase spindle structure (A), are seen. Cells displaying two dots are presumed to be the spindle pole bodies (SPBs) in early mitosis (EM). These EM dot-like structures are difficult to photograph, because they constantly move apart. Fluorescence at the cell equator in postanaphase cells is indicated by arrowheads. Bar, 10 μm. (*b*) Several examples of cells displaying anaphase spindle structures. Green fluorescence is uniform along the elongating rod. For the fully elongated spindles, the central region is often dim. Both spindle ends are intensely fluorescent, indicating that green fluorescence is localized at the SPBs. The aster microtubules (indicated by small arrows) are also green fluorescent. Fluorescence at the cell equator forming the ring is indicated by an arrowhead. Bar, 10 μm. (*c*) Green fluorescence in early or mid-mitotic cells. Fluorescence at the SPBs is intense. Bar, 10 μm. (*d*) Green fluorescence in control wild-type cells expressing GFP. Bar, 10 μm.

thetic medium, roughly half that reported previously at 36°C in a rich medium (Hiraoka et al. 1984). Fluorescence at the SPBs was strong throughout mitosis. Basically, the same video images were obtained for five mitotic cells examined.

Green fluorescence was also seen in the cell equator during late anaphase and postanaphase (indicated by arrowheads in Fig. 4a and b). It was reported recently that tubulin is enriched near the equator ring during anaphase and postanaphase (Pichová et al. 1995).

GFP-bound Dis1 in fixed cells

Green fluorescence could be still observed after cells were fixed with methanol and stained with DAPI (Fig. 6a). Cytoplasmic microtubular structures were seen to be basically the same as in nonfixed cells. The spindles were often not well preserved in methanol fixation (Hagan and Hyams 1988). The spindle microtubules were seen clearly only in cells with the dividing nucleus. Fluorescence at the SPB, however, became less visible in fixed cells. In glutaraldehyde-fixed cells (Fig. 6b), green fluorescence along cytoplasmic microtubules was very weak but the spindle staining was relatively uniform. Cells fixed with glutaraldehyde are known to have poorly preserved cytoplasmic microtubular structures (Hagan and Hyams 1988).

Localization of the carboxy-terminal fragment in mutant nuc2

As described above, the elevated dosage of the carboxy-terminal 31-kD fragment could substitute for the function of *dis1*$^+$. We addressed the question of whether this 31-kD fragment was capable of binding to microtubules or the SPBs. To this end, a plasmid containing the car-

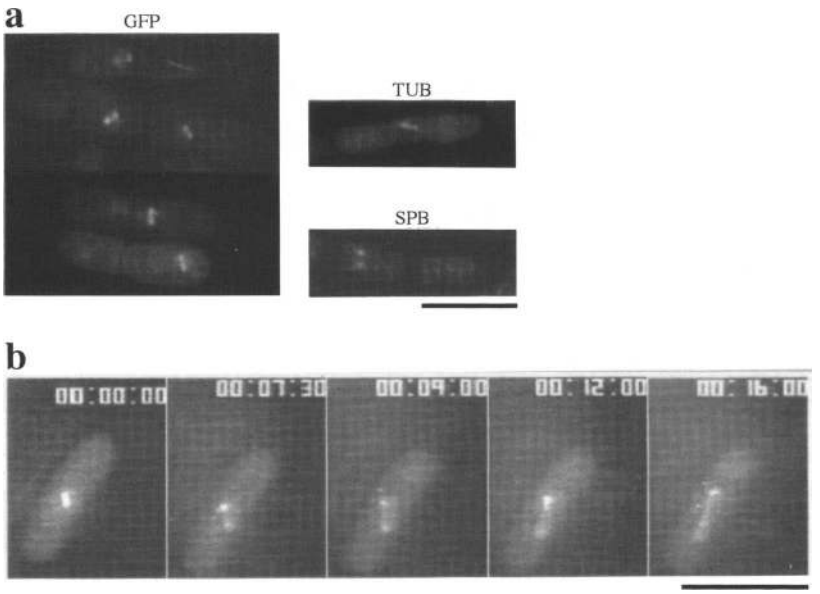

Figure 5. Localization of green fluorescence at the mitotic SPBs. (*a*) (*Left*) Green fluorescence in metaphase-arrested *nuc2* mutant cells carrying the plasmid pdis1–GFP and cultured at the restrictive temperature for 5 hr. Fluorescence at the SPBs is intense. (*Right*) *nuc2* mutant cells carrying pdis1–GFP were stained by anti-tubulin (TUB) or anti-sad1 (SPB) antibody and are shown for comparison. Bar, 10 μm. (*b*) Video images of a single mitotic cell taken by a Hamamatsu C1000 video camera. Green fluorescence at the SPBs is relatively strong, but that along the spindle microtubule is weak and minimal in metaphase. Green fluorescence is restored in the extended anaphase spindle. Bar, 10 μm.

boxy-terminal fragment ligated with GFP (pdis1Cter–GFP) was constructed and introduced into wild-type or mutant *nuc2* . This plasmid could complement the *dis1* null mutant phenotype, indicating that the GFP-bound 31-kD carboxy-terminal fragment was functional. In exponentially growing wild-type cells carrying the plasmid pdis1Cter–GFP, green fluorescence was not localized. Note that metaphase cells in wild-type culture constitute only 1%–2%, and the assignment of metaphase is difficult without anti-tubulin staining, which cannot be used simultaneously with the GFP method. However, in mitotically arrested *nuc2* mutant cells (36°C for 5 hr), >50% of which are in metaphase, green fluorescence was clearly accumulated around the SPBs (Fig. 7a). This green fluorescence at the SPBs was very weak so that it was recorded as the video images. The nucleus and the spindle displayed residual fluorescence. As a control, *nuc2* mutant cells expressing only GFP at the restrictive temperature are shown (Fig. 7b).

Phosphorylation of Cdc2 target sites in the central region in vivo

As an allele-specific cs mutation in the *dis2*$^{+}$ gene—which encodes a PP1 catalytic subunit—becomes lethal when combined with *dis1* mutations, p93^{dis1} may be regulated by phosphorylation and/or dephosphorylation. Phospholabeling experiments were performed to determine whether p93^{dis1} was phosphorylated in vivo. Extracts of ^{32}P-labeled *S. pombe* cells were prepared and boiled in 0.1% SDS for 3 min (see Materials and methods). Resulting solubilized extracts were clarified by centrifugation and immunoprecipitated by anti-dis1 antibodies (against the carboxyl terminus), followed by SDS-

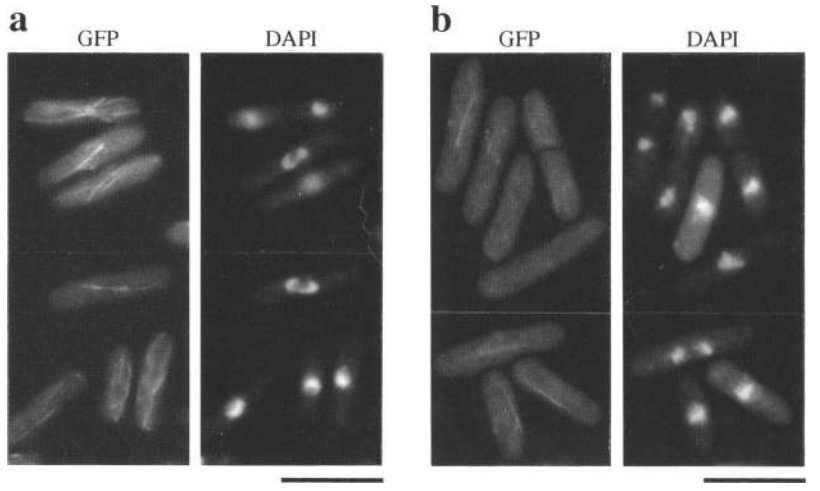

Figure 6. GFP-tagged Dis1 in fixed cells. (*a*) Green fluorescence (GFP) in cells fixed with methanol and stained with DAPI. Cytoplasmic microtubular structures were seen to be basically the same as in living cells. Green fluorescent spindle structures, which are often deformed, are seen in cells containing the dividing nucleus. Aster microtubules are also visible. Fluorescence at the SPB and the cell equator is much less apparent in fixed than in nonfixed cells. Bar, 10 μm. (*b*) Green fluorescence in glutaraldehyde-fixed cells is faint. Bar, 10 μm.

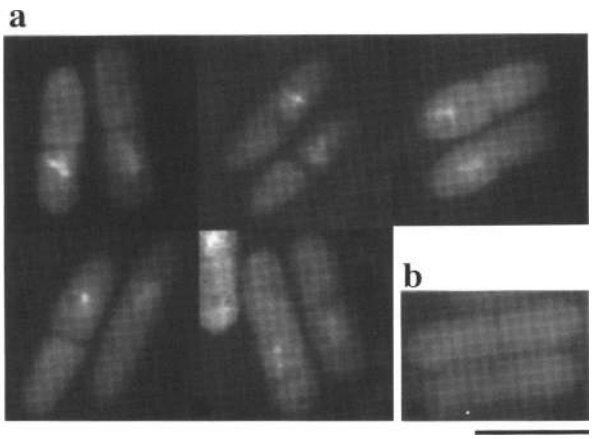

Figure 7. Green fluorescence localization by the carboxy-terminal 31-kD fragment. (*a*) Plasmid pdis1–Cter–GFP carrying the sequence coding for the carboxy-terminal 31-kD fragment bound to GFP was introduced into *nuc2* mutant cells and cultured at 36°C for 5 hr. Mitotically arrested cells showed weak green fluorescence, which was recorded by the highly sensitive video camera. Bar, 10 μm. (*b*) Green fluorescence in *nuc2* mutant cells expressing GFP at the restrictive temperature for 5 hr.

PAGE and autoradiography. $p93^{dis1}$ was phosphorylated in vivo (Fig. 8a). The 93-kD phosphoprotein band was observed in wild-type cells carrying the vector (lane 1) and the multicopy plasmid with the *dis1*$^+$ gene (lane 2), but not in the *dis1* gene disruptant (lane 3). When *dis1* deletion cells overproducing the *Bam*HI carboxy-terminal (Bam/C) fragment, which contained the carboxy-terminal half domain, were used (see Materials and methods), the 45-kD phosphorylated band was obtained (lane 4); the Bam/C region contained the phosphorylation site(s). Phosphoamino acid analysis of the fragment was performed, and phosphoserine was obtained (Fig. 8b).

To determine whether the serine residues in the putative Cdc2 targets of the Bam/C fragment were phosphorylated in vivo, alanine mutations were constructed and their phosphopeptide maps were compared. There are three Cdc2 consensus sites in the fragment. Triple and single mutants for three potential phosphorylation sites, S551, S556, and S590, were examined (Fig. 8c, top right). Immunoprecipitation of the triple mutant protein S551A S556A S590A showed that phospholabeling was reduced greatly.

In comparison to the phosphopeptide map of the wild-type Bam/C, which contained multiple spots, the three major spots (1, 2, and 3) were completely missing in the triple alanine mutant (Fig. 8c). Peptides found in single mutants indicated that spots 1, 2, and 3 were derived, respectively, from the peptides containing S551, S556, and S590 (Fig. 8c). The S551A mutation apparently affected the phosphorylation of S556. From these results we concluded that the $p93^{dis1}$ protein was multiply phosphorylated in vivo and that the phosphorylation sites included the three Cdc2 target sites present in the central domain.

Phosphorylation at the amino-terminal Cdc2 target sites

There are three additional Cdc2 target sites in the amino-terminal domain. We constructed a triple alanine mutant, T279A S293A S300A, in the full-length $p93^{dis1}$ and used it for in vivo labeling. These Cdc2 targets were also phosphorylated in vivo. This was shown by comparison of ^{32}P-labeled peptide mapping of $p93^{dis1}$ derived from wild type and the triple alanine mutant [Fig. 9; (left) full-length wild-type $p93^{dis1}$; (right) full-length triple alanine mutant N3A]. Three phosphopeptide spots (indicated by three small arrows) were missing in the alanine mutant protein; otherwise the peptide spots were identical. Hence, these Cdc2 target sites, T279, S293, and S300, in the amino-terminal domain and S551, S556, and S590 in the central domain are phosphorylated in vivo. There are several other minor sites. It remains to be determined whether these Cdc2 targets are actually phos-

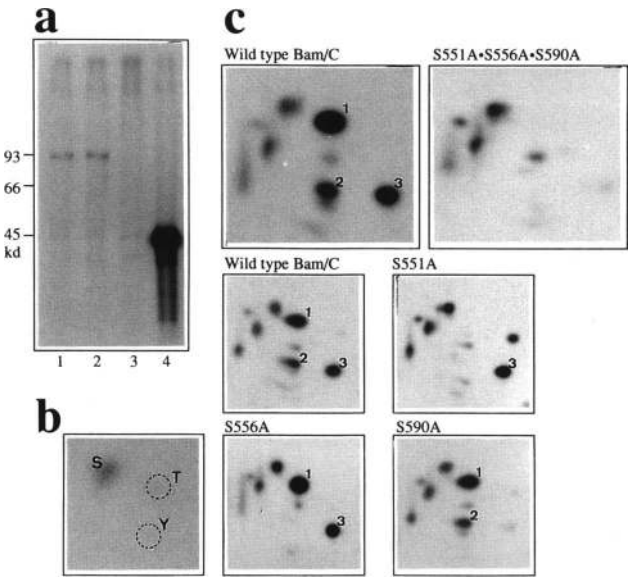

Figure 8. Phosphorylation of $p93^{dis1}$ at the Cdc2 target sites. (*a*) Phospholabeling was performed with wild-type cells carrying the vector plasmid (lane *1*) or a plasmid with the full-length *dis1*$^+$ gene (lane *2*), and gene disruptant cells carrying the vector (lane *3*) or a plasmid with the Bam/carboxy-terminal fragment, which is downstream of the nmt (no message in thiamine) promoter (Maundrell 1990) and overexpressed in the absence of thiamine (lane *4*). Immunoprecipitates were made by anti-dis1 antibodies, subjected to in SDS-PAGE, and autoradiographed. Immunoblotting of the same SDS–polyacrylamide gel with anti-dis1 antibodies showed band intensities roughly proportional to those of autoradiography (data not shown). (*b*) Phosphoamino acid analysis of the immunoprecipitates of p45 Bam/carboxy-terminal fragment. Phosphoserine was detected, as was a trace amount of phosphothreonine. (*c*) Phosphorylation of the wild-type and alanine mutants of the Bam/C fragment. Tryptic phosphopeptide maps of the wild-type, single, and triple alanine mutants are shown. Triple mutant S551A S556A S590A lacked three major phosphopeptides designated 1, 2, and 3. Single alanine mutants S551A, S556A, and S590A were also examined.

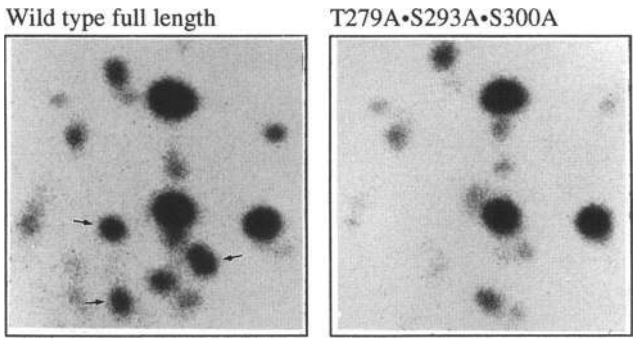

Figure 9. Phosphorylation of amino-terminal Cdc2 target sites. Phosphopeptide mapping of immunoprecipitated wild-type $p93^{dis1}$ and triple alanine mutant N3A protein (T279A S293A S300A) was done as described. Peptides indicated by arrows are missing in the N3A mutant protein. This mutant has alanine substitutions at T279, S293, and S300.

phorylated by Cdc2 kinase and dephosphorylated by PP1 phosphatases.

Discussion

Mitotic defects in dis1 *mutants*

Although Cdc2 kinase activity remains high in cs *dis1* mutant cells at the restrictive temperature, spindle elongation occurs in the absence of sister chromatid separation. The same phenotype is produced by the *dis1* deletion mutant made in the present study, indicating that the phenotype is not attributable to the leaky function of mutant protein. All the *dis1* mutants isolated so far contained nonsense mutations. The phenotype observed is therefore caused by loss of function.

Cell viability of *dis1* mutant sharply decreases during mitosis in the synchronous culture (Ohkura et al. 1988). This viability loss may be attributable to the untimely occurrence of spindle elongation. At the permissive temperature, *dis1* mutant cells show a mitotic delay phenotype; the frequency of cells having the short spindle increases fivefold compared with that in wild-type cultures (K. Nabeshima and M. Yanagida, unpubl.). This delay might be caused by the spindle checkpoint, negative feedback, or monitoring control (Hoyt et al. 1991; Li and Murray 1991; Spencer and Hieter 1992; Philp et al. 1993), possibly activated in response to the loss of $p93^{dis1}$. At the restrictive temperature, however, such control does not seem to be effective in mutant cells as spindle elongation is not inhibited.

Taken together, $p93^{dis1}$ is needed for sister chromatid separation, and its loss leads to the block of sister chromatid separation without blocking spindle elongation.

Dis1 interacts with microtubule

$p93^{dis1}$ is a novel microtubule-interacting protein; two pieces of evidence support this. First, immunofluorescence microscopy shows that $p93^{dis1}$ colocalizes with microtubules. Such antibody staining was completely lacking in *dis1*-disrupted cells, and was enhanced by a multicopy plasmid carrying the $dis1^+$ gene. Second, GFP-tagged Dis1 protein emits green fluorescence along cellular microtubule structures. The elongating spindle was seen clearly by green fluorescence of the GFP-tagged Dis1 protein.

The tagged GFP (Chalfie et al. 1994) is a powerful approach to identify the expressed proteins, and the present study confirms it as a valuable tool for visualizing protein localization in fission yeast cells. We have so far been able to observe four different fission yeast gene products using the GFP-tagging method and found they localized in a manner dependent on the genes used (S. Saitoh, and K. Kinoshita, unpubl.). GFP served as an excellent tag for protein localization as it was itself diffused in whole yeast cells. The GFP method reveals localization in living cells, which is an advantage over immunofluorescence microscopy. Certain protein–protein interactions may be clearly visualized only in intact cells. Alternatively, GFP tagging could be a potential source for producing artifactual images or inhibiting localization at a normal position. We conducted a number of control experiments to verify the green fluorescence observed to indicate the localization of Dis1 protein and to show that the GFP-tagged Dis1 is functional.

Green fluorescence of GFP-bound Dis1 protein is dim in the metaphase spindle microtubules. As Dis1 is clearly localized in anaphase spindle microtubules, Dis1 and/or its interacting component in the microtubules must differ between metaphase and anaphase. Dis1 considerably loses the ability to bind to microtubules in the Cdc2-activated metaphase stage. It remains to be determined whether $p93^{dis1}$ interacts directly with microtubules or how the interaction is regulated during cell cycle.

In vitro binding analysis using full-length and variously truncated Dis1 fragments made in bacteria showed that $p93^{dis1}$ bound to microtubule directly (Y. Nabeshima and M. Yanagida, unpubl.). The central domain essential for this interaction in vitro is rich in serine, threonine, proline, and basic amino acids. The microtubule-binding region found in certain microtubule-associating proteins (MAPs) such as MAP4 or tau (Aizawa et al. 1991; Kanai et al. 1992) is also rich in these amino acids. Three Cdc2 sites present in the central region of Dis1 may regulate association with microtubules. We showed that the sites are phosphorylated in vivo. However, it remains to be determined whether they are phosphorylated specifically in mitosis and phosphorylation affects binding to microtubules.

Interaction with the SPBs

The GFP-tagged Dis1 was clearly enriched at the SPBs during mitosis in living cells. As the SPB in G_2 phase or postanaphase (Funabiki et al. 1993; Hagan and Yanagida 1995) did not show green fluorescence, Dis1 seemed to have the affinity only for the mitotic SPBs in the spindle. GFP-tagged Dis1 in metaphase-arrested *nuc2* mutant

cells also displayed a strong signal at the SPBs. These results were different from antibody staining, which showed much weaker signal at the SPBs. Green fluorescence at the SPB was reduced after cells were fixed with methanol or glutaraldehyde, suggesting that association between Dis1 and the SPB was labile.

We reason that interaction with the mitotic SPBs is important in the execution of the role of $p93^{dis1}$. First, fluorescence at the SPB is enhanced specifically during mitosis. Time lapse video images of single mitotic cells confirm temporal accumulation of green fluorescence at the SPB from metaphase to anaphase. Second, the carboxy-terminal domain may be responsible for association with the SPBs, as the truncated carboxy-terminal 31-kD fragment is accumulated at the SPBs in *nuc2* mutant cells. The carboxy-terminal domain is functionally essential and its high dosage suppresses the *dis1* mutant phenotype.

The mitotic form of Dis1 protein may facilitate sister chromatid separation in anaphase A by interacting with components associating with the SPB . In *S. pombe*, cyclin B (Alfa et al. 1990) and a mitotic motor protein Cut7 (Hagan and Yanagida 1992) are known to associate specifically with the mitotic SPBs. Mutations in γ-tubulin (Horio et al. 1991) and a spindle formation protein Sad1 (Hagan and Yanagida 1995), which are constitutively bound to the SPB, show defects in spindle formation. In *A. nidulans*, BimA (Mirabito and Morris 1993), which is similar to fission yeast Nuc2 and budding yeast Cdc27, and γ-tubulin (Oakley 1992) also constitutively localize to the SPB. In *Saccharomyces cerevisiae*, a number of gene products essential for cell division cycle are known to bind to the SPBs (e.g., Spa1: Snyder and Davis 1988; Kar3: Meluh and Rose 1990; 80 kD: Rout and Kilmartin 1990; Cik1: Page and Snyder 1992; Nuf2: Osborne et al. 1994). A component to interact with Dis1 is likely to be an SPB protein modified in mitosis or to be associated only with the spindle SPBs.

The role of Dis1 protein in sister chromatid separation

The actual molecular function of $p93^{dis1}$ remains to be determined. Amino acid sequence of $p93^{dis1}$ is not very informative as it is a novel protein in the data bases. The amino-terminal domain, however, is considerably similar to the predicted sequence of a human cDNA with unknown function. At least a part of $p93^{dis1}$ is conserved. Because $p93^{dis1}$ interacts with microtubules, it may have a role in microtubule structure and function during the cell cycle. In fact, spindle extension timing is defective in *dis1* mutants in regard to its coordination with sister chromatid separation. In interphase, however, no defect in microtubular function has yet been identified. Cell viability of *dis1* mutants is retained until mitosis in the synchronous cultures. $p93^{dis1}$ is thus perhaps not needed in the G_2 phase, and interphase microtubules might serve as the dock for $p93^{dis1}$. Evidence derived from mutant analysis is consistent with this hypothesis. It is possible, however, that $p93^{dis1}$ has a certain redundant function in maintaining the interphase microtubule network.

How, then, does $p93^{dis1}$ function during mitosis? We presume that the localization shift of $p93^{dis1}$ in mitosis is important in understanding its role. Two types of shifts have been shown. First, fluorescence is shifted from microtubules to SPBs in the G_2/M progression. This type of shift can be explained by assuming that $p93^{dis1}$ is dissociated from microtubules upon the onset of mitosis, and a fraction of the dissociated $p93^{dis1}$ is moved to the SPBs. Dissociation from microtubules may be prerequisite for the execution of the $p93^{dis1}$ function in mitosis. Second, green fluorescence was shifted back to the spindle microtubules in anaphase. In the transition from metaphase to anaphase, at least a fraction of $p93^{dis1}$ acquires the ability to associate with spindle microtubules. It is not understood how anaphase spindle function is affected by association with $p93^{dis1}$. The spindle forms and elongates in *dis1* mutant cells. $p93^{dis1}$ may be implicated in anaphase spindle structure or its stability or degradation. In this case, $p93^{dis1}$ affects anaphase B as well as anaphase A. Alternatively, $p93^{dis1}$ may have no significant role in anaphase B; it simply moves back to its storage place (the microtubules) upon entry of the cell into anaphase.

The finding that the carboxy-terminal fragment alone is capable of associating with the SPBs and complementing the *dis1* phenotype suggests that the carboxy-terminal domain is related to sister chromatid separation. One hypothesis is that the amino-terminal half domain is regulatory for the carboxy-terminal function, whereas the central region acts to bind to microtubules. It is unknown how direct the role of $p93^{dis1}$ is in sister chromatid separation. It may control mitotic SPB function by direct interaction with the SPB or an SPB-associating component. Alternatively, it may be implicated in sister chromatid separation more indirectly through, for example, controlling components required for proteolysis (Holloway et al. 1993) or dephosphorylation (Stone et al. 1993), which are required for the onset of anaphase. A component for ubiquitin-dependent proteolysis has been shown recently to locate at the SPB-related centrosome and the spindle (Tugendreich et al. 1995; King et al. 1995).

Materials and methods

Strains, plasmids, cosmids, and media

Haploid *S. pombe* strains used were described previously (Ohkura et al. 1988: Kinoshita et al. 1993). For subcloning, pDB248 (Beach and Nurse 1981) and its derivative pSK248 were used. For nucleotide sequencing Bluescript KS(+)SK(−) (Stratagene, La Jolla, California) was used. The rich YPD and minimal EMM2 media were used (Mitchison 1970) for the culture of *S. pombe*.

Transformation, integration, and gene disruption

The lithium acetate method (Ito et al. 1983) was used for transformation of *S. pombe* cells. Integration of cloned sequences

into the chromosome by homologous recombination was performed by use of pYC11 and pYC12 (Chikashige et al. 1989). For gene disruption of *dis1*$^+$, a plasmid that carried the deleted *dis1* gene was made. An *Nde*I site was created at the initiation codon by site-directed mutagenesis. Then a 5-kb *Spe*I–*Pst*I fragment (*Pst*I and *Spe*I sites are located 0.85 kb upstream and 1.2 kb downstream of the initiation and termination codon of *dis1*$^+$, respectively) in Bluescript was digested with *Nde*I and *Eco*RI (an *Eco*RI site is situated 0.35 kb downstream of the termination codon). The *S. pombe ura4*$^+$ gene was then replaced with the *Nde*I–*Eco*RI fragment; the entire coding region was replaced with the marker gene. The resulting plasmid was linearized with *Spe*I and *Pst*I and used for transformation of an *S. pombe* diploid CL31/6 (*h*$^+$/*h*$^-$ *leu1/leu1 ura4/ura4 ade6-210/ade6-216 lys1/+*). Stable transformants obtained were analyzed by tetrads. Genomic DNAs of diploids and segregants were prepared, and gene disruption at the expected places was verified by Southern hybridization.

Construction of a cosmid library of S. pombe *genomic DNA*

A cosmid library for *S. pombe* genomic DNA was made by use of the procedure of Evans et al. (1989). Large genomic DNA (average length, about 300 kb) of *S. pombe* (Matsumoto et al. 1987) was partially digested by *Sau*3AI (0.01 U/μg of genomic DNA, 36°C for 30 min) and ligated by use of T4 DNA ligase with sCosl–LEU2 cleaved previously by *Bam*HI and *Xho*I. sCosl–LEU2 was constructed by ligation of the *S. cerevisiae LEU2* gene with the unique *Hin*dIII site of sCosl (Evans et al. 1989) and was the kind gift of Dr. T. Matsumoto (Albert Einstein College of Medicine, The Bronx, NY). The cosmid library was made by in vitro packaging using Gigapack Gold (Stratagene).

Isolation of the dis1$^+$ *gene*

The *dis1* locus had a weak linkage to *ura4* (~40 cM), and chromosome walking was employed to isolate the *dis1*$^+$ gene. The initial marker for hybridization was the *ura4*$^+$ gene. To estimate the genetic distances between the *ura4* locus and the cloned DNAs, subcloned DNAs were integrated onto the chromosome with the marker gene (the *S. cerevisiae LEU2*). Cosmid walking was done in two directions with the *ura4*$^+$ gene as the initial probe (Yanagida et al. 1991). DNAs with a total length of 300 kb obtained by chromosome walk with 15 probes were ordered by the cosmid clones obtained. By integration of subclones with the marker gene onto the chromosome, one fragment, ~200 kb apart from *ura4*$^+$, was found to be tightly (2.4 cM) linked to the *dis1* locus. Cosmid DNAs containing that fragment could complement cs *dis1* mutants. By subcloning followed by nucleotide sequencing, the *dis1*$^+$ gene was identified. cDNA clones were isolated to verify the coding region and the presence of an intron. The genomic and cDNA clones fully restored cs phenotype when introduced into cs *dis1* mutant cells.

Isolation of cDNA

An *S. pombe* cDNA library (the gift of Dr. M. Wigler) was used for screening cDNA clones for the *dis1*$^+$ gene by plaque hybridization. Five phage clones (pCK100, 200, 300, 400, and 500) were obtained, and partially sequenced. Four of them contained the full-length coding region. The noncoding 5′ sequence in one cDNA clone was more than 1 kb long, whereas remaining cDNA clones were 150–200 bp long. The noncoding 3′ sequences were ~200 bp.

Construction of the fused protein and preparation of antiserum

Plasmid pAR3039 (Studier and Moffat 1986) was used for expression of the *dis1*$^+$-coding region in the bacterial strain BL21. The 1-kb *Spe*I–*Eco*RI fragment was ligated with the plasmid, and the resulting pARDIS1 caused the synthesis of a large quantity of a 31-kD protein in bacterial cells induced by IPTG. This carboxy-terminal fragment was purified by a previously described procedure (Watt et al. 1985), and 200 μg of polypeptide was injected into a rabbit each time by the procedures described (Hirano et al. 1988).

Immunochemical methods

Immunoprecipitation with *S. pombe* extracts and affinity purification of antibodies were done as described previously (Yamano et al. 1994). Antibodies were mixed with Protein A–sepharose beads (Pharmacia) for 2 hr at room temperature with shaking, followed by washing. The supernatant extracts were added and incubated at 4°C for 4–6 hr with shaking; this was followed by six washings and SDS-PAGE after boiling for 3 min. Immunoblotting was performed as described (Towbin et al. 1979).

In vivo labeling

The method of Simanis and Nurse (1986) was followed with modifications (Shiozaki and Yanagida 1992: Yamano et al. 1994). *S. pombe* cells were grown at 33°C in synthetic EMM1 medium (Mitchison 1970) to a cell concentration of 2×10^6 to 3×10^6/ml; $H_3{}^{32}PO_4$ (1 mCi) was added to the 10-ml cultures and incubated with shaking for 3 hr. Labeled cells were washed and broken with glass beads. Resulting extracts were boiled with 0.1% SDS for 3 min, left on ice for 30 min, and centrifuged at 14,000 rpm for 20 min; supernatants were used for immunoprecipitation after addition of NP-40 and sodium deoxycholate (final concentration 0.5%).

Construction of alanine mutants

A procedure similar to that described by Yamano et al. (1994) was followed. A 0.4-kb *Bam*HI–*Spe*I fragment was subcloned into Bluescript and mutagenized by use of the in vitro mutagenesis system (Amersham). Oligonucleotides were made to construct mutants S551A, S556A, and S590A. The wild-type *Bam*HI–*Spe*I in pREP41–dis1 (full length) and pREP41–Bam/C were replaced, respectively, with the mutagenized fragments. For N3A mutant, the 0.4-kb *Hin*dIII–*Kpn*I fragment was mutagenized. Oligonucleotides were made to construct T279A, S293A, and S300A. The wild-type *Hin*dIII–*Kpn*I fragment of pREP1–dis1 (full length) was replaced with the mutagenized fragment. Nucleotide sequences of resulting mutant clones were determined by use of a Dye Deoxy Cycle sequencing kit (Applied Biosystems Inc., Foster City, CA).

Phosphoamino acid analysis and tryptic phosphopeptide mapping

Procedures described previously (Shiozaki and Yanagida 1992; Yamano et al. 1994) were followed. ^{32}P-Labeled protein was immunoprecipitated, run in SDS-PAGE, and transferred to Immobilon (Millipore). A slice of Immobilon containing the ^{32}P-labeled protein was subjected to acid hydrolysis or two-dimensional tryptic phosphopeptide mapping (Boyle et al. 1991). The hydrolysate was subjected to electrophoresis (first run, pH 1.9, 1.5 kV for 20 min; second run, pH 3.5, 1.3 kV for 16 min). For

tryptic mapping, the samples were dissolved in electrophoresis buffer after lyophilization (50 ml of *n*-butanol, 25 ml of acetic acid, 900 ml of H_2O, 25 ml of pyridine at pH 4.7). A count of 500–1000 cpm phosphopeptides was developed two dimensionally on a cellulose thin-layer plate (20×20 cm): The first dimension involved electrophoresis at 1 kV for 40 min, and the second dimension, ascending chromatography (75 ml of *n*-butanol, 15 ml of acetic acid, 60 ml of H_2O, 50 ml of pyridine).

PFG electrophoresis, Southern blotting, and nucleotide sequencing

The standard procedures for Southern, colony, and plaque hybridization were followed (Maniatis et al. 1982). The dideoxy method (Sanger et al. 1977) was employed for nucleotide sequencing with stepwise deletion (Yanisch-Perron et al. 1985).

Fluorescence and immunofluorescence microscopy

For immunofluorescence microscopy, the procedures described by Hagan and Hyams (1988) were followed. Anti-tubulin antibody (TAT-1) was described previously by Woods et al. (1989). Affinity-purified anti-dis1 antibodies were also used. For DAPI staining, *S. pombe* cells were fixed in 2.5% glutaraldehyde at 33°C for 20–30 min.

Expression of Dis1 with the carboxyl terminus tagged with GFP

Plasmid TU#65 (Chalfie et al. 1994) was employed to construct the *dis1*$^+$ gene with the carboxyl terminus tagged with GFP. The resulting plasmid, pGP120, contains an ~2-kb-long 5′-upstream sequence containing the native promoter, the full-length coding region of *dis1*$^+$ with the carboxyl terminus ligated to the GFP sequence in frame. In addition, the marker gene *S. cerevisiae leu2* and the *S. pombe* replication origin ARS1 are present. pGP120 was introduced into the *dis1* null mutant (*h*$^-$ *leu1 ura4 dis1::Ura4*). The expected size of the fusion polypeptide (120 kD) was detected in transformants, the level of which was four- or fivefold higher than that of wild-type p93^{dis1} (data not shown).

Observation of green fluorescent Dis1 protein in S. pombe *cells*

dis1-deletion mutant cells carrying pGP120 were cultured at 33°C in EMM2 to log phase, mounted directly on a slide glass without fixation, covered with a coverslip, and observed by a Zeiss Axiophot microscope according to Chalfie et al. (1994). Zeiss blue–violet and blue filter sets were used. For fixation, cells were treated with methanol for 8 min at −80°C or with 2.5% glutaraldehyde at 33°C for 1 hr. *nuc2-663* mutant cells (*h*$^-$ *leu1 nuc2-663*) transformed with pGP120 were cultured at 26°C in EMM2 to 4×10^6/ml and then transferred at 36°C for 5 hr. Video images were generated by a C1000 type 12 Hamamatsu SIT video camera. Cells were illuminated for 2–3 sec with a 30-sec interval and recorded.

Acknowledgments

We thank Drs. K. Gull and Y. Nagahama for the gifts of antibodies, Drs. M. Chalfie and M. Wigler for plasmids and cDNA library, and Dr. P. Nurse for reading an early draft and comments on the manuscript. This work was supported by grants from the Ministry of Education, Science, and Culture of Japan (specially promoted research) and the Human Frontier Science Program Organization.

The publication costs of this article were defrayed in part by payment of page charges. This article must therefore be hereby marked "advertisement" in accordance with 18 USC section 1734 solely to indicate this fact.

References

Aizawa, H., Y. Emori, A. Mori, H. Murofushi, H. Sakai, and K. Suzuki. 1991. Functional analyses of the domain structure of microtubule-associated protein-4 (MAP-U). *J. Biol. Chem.* **266:** 9841–9846.

Alfa, C.E., B. Ducommun, D. Beach, and J.S. Hyams. (1990). Distinct nuclear and spindle pole body populations of cyclin-cdc2 in fission yeast. *Nature* **347:** 680–682.

Axton, J.M., V. Dombradi, P.T.W. Cohen, and D.M. Glover. 1990. One of the protein phosphatase 1 isozymes in *Drosophila* is essential for mitosis. *Cell* **63:** 33–46.

Beach, D. and P. Nurse. 1981. High-frequency transformation of the fission yeast *Schizosaccharomyces pombe*. *Nature* **290:** 140–142.

Belmont, L.D., A.A. Hyman, K.E. Sawin, and T.J. Mitchison. 1990. Real-time visualization of cell cycle-dependent changes in microtubule dynamics in cytoplasmic extracts. *Cell* **62:** 579–589.

Bergen, L.G., R. Kuriyama, and G.G. Borisy. 1980. Polarity of microtubules nucleated by centrosomes and chromosomes of Chinese hamster ovary cells in vitro. *J. Cell Biol.* **50:** 416–431.

Boyle, W.J., P.V. Geer, and T. Hunter. 1991. Phosphopeptide mapping and phosphoamino acid analysis by two-dimensional separation on thin-layer cellulose plates. *Methods Enzymol.* **201:** 110–149.

Chalfie, M., Y. Tu, G. Euskirchen, W.W. Ward, and D.C. Prasher. 1994. Green fluorescent protein as a marker for gene expression. *Science* **263:** 802–805.

Chikashige, Y., N. Kinoshita, Y. Nakaseko, T. Matsumoto, S. Murakami, O. Niwa, and M. Yanagida. 1989. Composite motifs and repeat symmetry in *S. pombe* centromeres: direct analysis by integration of NotI restriction sites. *Cell* **57:** 739–751.

Ding, R., K.L. McDonald, and J.R. McIntosh. 1993. Three-dimensional reconstruction and analysis of mitotic spindles from the yeast, *Schizosaccharomyces pombe*. *J. Cell Biol.* **120:** 141–152.

Doonan, J.H. and N.R. Morris. 1989. The *bimG* gene of *Aspergillus*, required for completion of anaphase encodes a homolog of mammalian phosphoprotein phosphatase 1. *Cell* **57:** 987–996.

Evans, G.A., K. Lewis, and B.E. Rothenberg. 1989. High efficiency vectors for cosmid microcloning and genomic analysis. *Gene* **79:** 9–20.

Funabiki, H., I. Hagan, S. Uzawa, and M. Yanagida. 1993. Cell cycle-dependent specific positioning and clustering of centromeres and telomeres in fission yeast. *J. Cell Biol.* **121:** 961–976.

Gliksman, N.R., S.F. Parsons, and E.D. Salmon. 1992. Okadaic acid induces interphase to mitotic-like microtubule dynamic instability by inactivating rescue. *J. Cell Biol.* **119:** 1271–1276.

Hagan, I. and J.S. Hyams. 1988. The use of cell division cycle mutants to investigate the control of microtubule distribution in the fission yeast *Schizosaccharomyces pombe*. *J. Cell Sci.* **89:** 343–357.

Hagan, I.M. and M. Yanagida. 1992. Kinesin-related cut7 protein associates with mitotic and meiotic spindles in fission yeast. *Nature* **356:** 74–76.

———. 1995. The product of the spindle formation gene sad1$^+$ associates with the fission yeast spindle pole body and is essential for viability. *J. Cell Biol.* **129:** 1033–1047.

Heidemann S.R. and J.R. McIntosh. 1980. Visualization of the structural polarity of microtubules. *J. Cell Biol.* **286:** 517–519.

Hirano, T., Y. Hiraoka, and M. Yanagida. 1988. A temperature sensitive mutation of the *S. pombe* gene *nuc2*$^+$ that encodes a nuclear scaffold-like protein blocks spindle elongation in mitotic anaphase. *J. Cell Biol.* **106:** 1171–1183.

Hiraoka, Y., T. Toda, and M. Yanagida. 1984. The *NDA3* gene of fission yeast encodes β-tubulin: A cold sensitive *nda3* mutation reversibly blocks spindle formation and chromosome movement in mitosis. *Cell* **39:** 349–358.

Holloway, S., M. Glotzer, R.W. King, and A.W. Murray. 1993. Anaphase is initiated by proteolysis rather than by the inactivation of maturation-promoting factor. *Cell* **73:** 1393–1402.

Horio, T., S. Uzawa, M.K. Jung, B.R. Oakley, K. Tanaka, and M. Yanagida. 1991. The fission yeast γ-tubulin is essential for mitosis and is localized at microtubule organizing centers. *J. Cell Sci.* **99:** 693–700.

Hoyt, M.A., L. Totis, and B.T. Roberts. 1991. *S. cerevisiae* genes required for cell cycle arrest in response to loss of microtubule function. *Cell* **66:** 507–517.

Ito, H., Y. Fukuda, K. Murata, and A. Kimura. 1983. Transformation of intact yeast cells treated with alkali cations. *J. Bacteriol.* **153:** 163–168.

Kanai, Y., J. Chen, and N. Hirokawa. 1992. Microtubule bundling by tau proteins in vivo: Analysis of functional domains. *EMBO J.* **11:** 3953–3961.

King, R.W., J.-M. Peters, S. Tugendreich, M. Rolfe, P. Hieter, and M.W. Kirschner. 1995. A 20S complex containing CDC27 and CDC16 catalyzes the mitosis-specific conjugation of ubiquitin to cyclin B. *Cell* **81:** 279–288.

Kinoshita, N., H. Ohkura, and M. Yanagida. 1990. Distinct, essential roles of type 1 and 2A protein phosphatases in the control of the fission yeast cell division cycle. *Cell* **63:** 405–415.

Kinoshita, N., H. Yamano, F. Le Bouffant-Sladeczk, H. Kurooka, H. Ohkura, E.M. Stone, M. Takeuchi, T. Toda, T. Yoshida, and M. Yanagida. 1991a. Sister-chromatid separation and protein dephosphorylation in mitosis. *Cold Spring Harbor Symp. Quant. Biol.* **56:** 621–628.

Kinoshita, N., M. Goebl, and M. Yanagida. 1991b. The fission yeast *dis3*$^+$ gene encodes a 110-kDa essential protein implicated in mitotic control. *Mol. Cell. Biol.* **11:** 5839–5847.

Kinoshita, N., H. Yamano, H. Niwa, T. Yoshida, and M. Yanagida. 1993. Negative Regulation of mitosis by fission yeast protein phosphatase ppa2. *Genes & Dev.* **7:** 1059–1071.

Li, R. and A. Murray. 1991. Feedback control of mitosis in budding yeast. *Cell* **66:** 519–531.

Maniatis, T., E.F. Fritsch, and J. Sambrook. 1982. *Molecular cloning: A laboratory manual.* Cold Spring Harbor Laboratory, Cold Spring Harbor, New York.

Masuda, H., M. Sevik, and Z. Cande. 1992. *In vitro* microtubule-nucleating activity of spindle pole bodies in fission yeast *Schizosaccharomyces pombe*: Cell cycle dependent activation in *Xenopus* cell-free extracts. *J. Cell Biol.* **117:** 1055–1066.

Matsumoto, T., K. Fukui, O. Niwa, N. Sugawara, J. W. Szostak, and M. Yanagida. 1987. Identification of healed terminal DNA fragments in linear minichromosomes of *Schizosaccharomyces pombe*. *Mol. Cell Biol.* **7:** 4424–4430.

Maundrell, K. 1990. nmt1 of fission yeast. *J. Biol. Chem.* **265:** 10857–10864.

Mayer-Jaekel, R., H. Ohkura, R. Gomes, C.E. Sunkel, S. Baumgartner, B.A. Hemmings, and D.M. Glover. 1993. The 55 kd regulatory subunit of Drosophila protein phosphatase 2A is required for anaphase. *Cell* **72:** 621–633.

McCully, E.K. and C.F. Robinow. 1971. Mitosis in the fission yeast *Schizosaccharomyces pombe*: A comparative study with light and electron microscopy. *J. Cell Sci.* **9:** 475–507.

McNally, F.J. and R.D. Vale. 1993. Identification of katanin, an ATPase that severs and disassembles stable microtubules. *Cell* **75:** 419–429.

Meluh, P.B. and M.D. Rose. 1990. KAR3, a kinesin-related gene required for yeast nuclear fusion. *Cell* **60:** 1029–1041.

Mirabito, P.M. and N.R. Morris. 1993. BIMA, a TPR-containing protein required for mitosis, localizes to the spindle pole body in *Aspergillus nidulans*. *J. Cell Biol.* **120:** 959–968.

Mitchison, J.M. 1970. Physiological and cytological methods for *Schizosaccahromyces pombe*. *Methods Cell. Physiol.* **4:** 131–165.

Mitchison, T. and M. Kirschner. 1984. Dynamic instability of microtubule growth. *Nature* **312:** 237–242.

Nurse, P. 1990. Universal control mechanism regulating onset of M-phase. *Nature* **344:** 503–508.

Oakley, B.R. 1992. γ-Tubulin: The microtubule organizer? *Trends Cell Biol.* **2:** 1–6.

Ohkura, H., Y. Adachi, N. Kinoshita, O. Niwa, T. Toda, and M. Yanagida. 1988. Cold-sensitive and caffeine supersensitive mutants of the *Schizosaccharomyces pombe* dis genes implicated in sister chromatid separation during mitosis. *EMBO J.* **7:** 1465–1473.

Ohkura, H., N. Kinoshita, S. Miyatani, T. Toda, and M. Yanagida. 1989. The fission yeast *dis2*$^+$ gene required for chromosome disjoining encodes one of two putative type1 protein phosphatases. *Cell* **57:** 997–1007.

Osborne, M.A., G. Schlenstedt, T. Jinks, and P.A. Silver. 1994. Nuf2, a spindle pole body associated protein required for nuclear division in yeast. *J. Cell Biol.* **125:** 853–866.

Page, B. and M. Snyder. 1992. CIK1: A developmentally regulated sindle pole body-associated protein important for microtubule functions in *Saccharomyces cerevisiae*. *Genes & Dev.* **6:** 1414–1429.

Philip, A.V., J.M. Axton, R.D. Saunders, and D.M. Glover. 1993. Mutations in the Drosophila melanogaster gene three rows permit aspects of mitosis to continue in the absence of chromatid segregation. *J. Cell Sci.* **106:** 87–98.

Pichová, A., S.D. Kohlwein, and M. Yamamoto. 1995. New arrays of cytoplasmic microtubules in the fission yeast *Schizosaccharomyces pombe*. *Protoplasma* (in press).

Rout, M.P. and J.V. Kilmartin. 1990. Components of the yeast spindle and spindle pole body. *J. Cell Biol.* **111:** 1913–1927.

Sanger, F., S. Nicklen, and A.R. Coulson. 1977. DNA sequencing with chain-terminating inhibitors. *Proc. Natl. Acad. Sci.* **74:** 5463–5467.

Shiina, N., Y. Gotoh, N. Kubomura, A. Iwamatsu, and E. Nishida. 1994. Microtubule severing by elongation factor 1α. *Science* **266:** 282–285.

Shimanuki, M., N. Kinoshita, H. Ohkura, T. Yoshida, T. Toda, and M. Yanagida. 1993. Isolation and characterization of the fission yeast protein phosphatase gene *ppe1*$^+$ involved in cell shape control and mitosis. *Mol. Biol. Cell.* **4:** 303–313.

Shiozaki, K. and M. Yanagida. 1992. Functional dissection of the phosphorylated termini of fission yeast DNA topoisomerase II. *J. Cell Biol.* **119:** 1023–1036.

Simanis, V. and P. Nurse. 1986. The cell cycle control gene

cdc2$^+$ of fission yeast encodes a protein kinase potentially regulated by phosphorylation. *Cell* **45:** 261–268.

Snyder, M. 1994. The spindle pole body of yeast. *Chromosoma* **103:** 369–380.

Snyder, M. and R.W. Davis. 1988. SPA1: A gene important for chromosome segregation and other mitotic functions in *S. cerevisiae*. *Cell* **54:** 743–754.

Spencer, F. and P. Hieter. 1992. Centromere DNA mutation induce a mitotic delay in *Saccharomyces cerevisiae*. *Proc. Natl. Acad. Sci.* **89:** 8908–8912.

Stone, E.M., H. Yamano, N. Kinoshita, and M. Yanagida. 1993. Mitotic regulation of protein phosphatases by the fission yeast sds22 protein. *Curr. Biol.* **3:** 13–26.

Studier, F.W. and B.A. Moffat. 1986. Use of bacteriophage T7 RNA polymerase to direct selective high-level expression of cloned genes. *J. Mol. Biol.* **189:** 113–130.

Takeuchi, M. and M. Yanagida. 1993. A mitotic role for a novel fission yeast protein kinase dsk1 with cell cycle stage dependent phosphorylation and localization. *Mol. Biol. Cell.* **4:** 247–260.

Tanaka, K. and T. Kanbe. 1986. Mitosis in the fission yeast *Schizosaccharomyces pombe* as revealed by freeze-substitution electron microscopy. *J. Cell Sci.* **80:** 253–268.

Towbin, H., T. Staehelin, and J. Gordon. 1979. Electrophoretic transfer of proteins from polyacrylamide gels to nitrocellulose sheets; procedure and some applications. *Proc. Natl. Acad. Sci.* **76:** 4350–4354.

Tugendreich, S., J. Tomkiel, W. Earnshaw, and P. Hieter. 1995. The CDC27HS protein co-localizes with the CDC16HS protein to the centrosome and mitotic spindle and is essential for the mataphase to anaphase transition. *Cell* **81:** 261–268.

Vale, R.D. 1991. Severing of stable microtubules by a mitotically activated protein in Xenopus egg extracts. *Cell* **64:** 827–839.

Vandré, D.D. and V.L. Wills. 1992. Inhibition of mitosis by okadaic acid: Possible involvement of a protein phosphatase 2A in the transition from metaphase to anaphase. *J. Cell Sci.* **101:** 79–91.

Verde, F., M. Dogterom, E. Stelzer, E. Karsenti, and S. Leibler. 1992. Control of microtubule dynamics and length by cyclin A- and cyclin B-dependent kinases in *Xenopus* egg extracts. *J. Cell Biol.* **118:** 1097–1108.

Walker, R.A., E.T. O'Brien, N.K. Pryer, M.F. Sobeiro, W.A. Voter, H.P. Erickson, and E.D. Salomon. 1988. Dynamic instability of individual microtubules analyzed by video light microscopy: Rate constants and transition frequencies. *J. Cell Biol.* **107:** 1437–1448.

Watt, R.A., A.R. Shatzman, and M. Rosenberg. 1985. Expression and characterization of the human c-myc DNA-binding protein. *Mol. Cell Biol.* **5:** 448–456.

Woods, A., T. Sherwin, R. Sasse, T.H. McRae, A.J. Baines, and K. Gull. (1989). Definition of individual components within the cytoskeleton of *Trypanosoma brucei* by a library of monoclonal antibodies. *J. Cell Sci.* **93:** 491–500.

Yamano, H., K. Ishii, and M. Yanagida. 1994. Phosphorylation of dis2 protein phosphatase at the C-terminal cdc2 consensus and its potential role in cell cycle regulation. *EMBO J.* **13:** 5310–5318.

Yanagida, M., O. Niwa, Y. Chikashige, T. Matsumoto, S. Murakami, H. Kurooka, T. Horio, and M. Shimanuki. 1991. Genome analysis of *Schizosaccharomyces pombe*. In *Control of cell growth and division*. (ed. A. Ishihama and H. Yoshikawa), pp. 255–262. Japan Sci. Soc. Press/Springer-Verlag, Tokyo, Japan.

Yanisch-Perron, C., J. Vieria, and J. Messing. 1985. Improved M13 phage cloning vectors and host strains: Nucleotide sequences of the M13m18 and pUC19 vectors. *Gene* **33:** 103–119.

p93dis1, which is required for sister chromatid separation, is a novel microtubule and spindle pole body-associating protein phosphorylated at the Cdc2 target sites.

K Nabeshima, H Kurooka, M Takeuchi, et al.

Genes Dev. 1995, **9:**
Access the most recent version at doi:10.1101/gad.9.13.1572